

## IMPROVEMENT THE THERMAL PERFORMANCE OF MYRISTIC ACID

Mehmet Akif Ezan\*, Seyma Ince, Yoldas Seki, Alpaslan Turgut, Levent Cetin, Aytunc Ereğ

\*Author for correspondence

Department of Mechanical Engineering,

Dokuz Eylül University,

Izmir, Turkey,

E-mail: [mehmet.ezan@deu.edu.tr](mailto:mehmet.ezan@deu.edu.tr)

### ABSTRACT

This study mainly focus on two aspects; the first one is to increase the thermal conductivity of Myristic acid with graphene additives and the second one is to determine the influence of this increment on the melting duration of a particular encapsulated thermal energy storage system with PCM. As a result, thermal conductivity of composite myristic acid increased by 8%, 18% and 38% after graphene loadings of 0.5%, 1% and 2% into the pure MA, respectively. Besides, one-dimensional spherical computational domain has been considered, and the conduction dominated phase change process simulated with implementing temperature transformation method. Validity of the current code has been revealed by reproducing a numerical work in literature. For this particular case, it is found that the increments of 8%, 18% and 38% in thermal conductivity tend to reduce the total time of melting by 5.6%, 15% and 26%.

### INTRODUCTION

Phase change materials are used to provide sustainable usage of thermal energy in widespread applications. The major advantage of a thermal system with PCMs is that, a great amount of a thermal energy can be stored inside the system or an auxiliary storage tank while the demand is low and then discharged when the energy source is not available, or the demand exceeds the capacity of the system [1, 2]. Since the solidification or melting process takes place almost at a constant temperature, a system with PCM will act as an energy source at a predefined temperature range. One of the most well-known examples for this kind of thermal energy shifting application is storing the solar energy during the daytime and then re-using it at night time when the solar power is not available.

Among the wide range of possible PCMs, fatty acids are one of the most appropriate candidates for using at moderate temperature applications (20°C to 100°C), since they are cheap, widely available, thermally stable and most importantly they are not harmful to human body or nature [3].

### NOMENCLATURE

$Bi$	[-]	Biot number
$c$	[J/kgK]	Specific heat
$C$	[-]	Dimensionless heat capacity
$C^*$	[J/m <sup>3</sup> K]	Volumetric heat capacity
$F_c$	[%]	Crystallinity
$h$	[W/m <sup>2</sup> K]	Heat transfer coefficient
$H$	[J/m <sup>3</sup> ]	Total enthalpy per volume
$k$	[W/mK]	Thermal conductivity
$K$	[-]	Dimensionless thermal conductivity
$r$	[m]	Radial axis direction
$R$	[-]	Dimensionless radial axis
$T$	[°C]	Temperature
$s$	[Jm <sup>3</sup> /kg]	Source term
$S$	[-]	Dimensionless source term
$S^*$	[J/m <sup>3</sup> ]	Source term per volume
$Ste$	[-]	Stefan number
$t$	[s]	Time

#### Special characters

$\alpha$	[m <sup>2</sup> /s]	Thermal diffusivity
$\varepsilon$	[-]	Convergence criteria
$\delta r$	[mm]	Wall thickness of sphere
$\delta T_m$	[°C]	Temperature range of mushy zone
$\delta \theta_m$	[-]	Dimensionless temperature range of mushy zone
$\Delta H$	[J/kg]	Latent heat of fusion
$\rho$	[kg/m <sup>3</sup> ]	Density
$\theta$	[-]	Dimensionless temperature
$\tau$	[-]	Dimensionless time

#### Subscripts

$f$	Freezing
$in$	Initial
$L$	Liquid phase
$m$	Melting or Mushy region
$o$	Outer
$S$	Solid phase

Sharma et al. [3] also indicated that fatty acids have higher heat of fusion values comparable to paraffin's. Unlike the most of salt hydrates, the melting/solidification behaviour of fatty acids is quite stable such that, they do not have problems such as phase segregation or sub-cooling. Besides, the major

drawback of fatty acids is that their thermal conductivity values are lower comparing to the other types of PCMs [4].

There are many studies that focus on enhancement of the thermal properties of fatty acids with novel additives. Sari et al. [5] prepared fatty acid/expanded graphite (EG) composite PCMs. They have considered capric acid (CA), lauric acid (LA) and myristic acid (MA) as pure PCMs in the preparation of composites. In addition to the DSC and SEM analyses, they have also carried out an experimental work within a constant temperature bath to compare the melting and solidification durations of pure and composite PCMs. Results show that the phase change temperatures of composite PCMs remain almost constant comparing to the pure PCMs, but the latent heat of fusion values decrease more than 20% for all cases. It is also reported that, solidification durations of CA/EG, LA/EG and MA/EG composite PCMs were reduced by 68%, 33% and 56% respectively, comparing the pure ones. Similarly, in terms of the melting durations, reductions of 17%, 22% and 53% were observed for CA/EG, LA/EG and MA/EG composite PCMs, respectively.

Fauzi et al. [6] considered myristic acid/palmitic acid (MA/PA) eutectic mixture as a PCM. They have prepared composite PCMs with adding sodium myristate (SM), sodium palmitate (SP), and sodium stearate (SS) into the MA/PA eutectic mixture. It is indicated that with the addition of 5% SM, 5% SP, and 5% SS into the MA/PA mixture, while the degree of sub-cooling was decreased, the thermal conductivity and the amount of latent heat of fusion were increased.

Mehrali et al. [7] investigated palmitic acid/graphene nanoplatelets (PA/GNPs) as a composite PCM. They have prepared a shape stable composite PCM, which means that PA was absorbed by GNPs so that there is no leakage of PA at the end of discharging period. Results indicate that the thermal conductivity value of the PA/GNPs composite with 77.99% (wt.) of PA is 10 times higher than the pure PA. Experimental findings also reveal that, while the pure PA needs 360 s to reach the phase change temperature, the time is needed for the PA/GNPs composite with 77.99% (wt.) PA is only 150 s.

This study mainly aims to enhance the thermal conductivity of myristic acid (MA), with keeping the remaining thermal properties unchanged. For this purpose, graphene is added at various ratios (0.5%, 1%, and 2%) into the MA. Thermal characterization of the composite PCMs is conducted by using Differential scanning calorimeter (DSC), and Thermo gravimetric analysis (TGA). Thermal cycling tests are also performed to investigate the long term chemical and thermal stabilities of the composite PCMs. Moreover, a comparative numerical study is presented to introduce the effect of thermal conductivity on the melting duration of composite PCMs.

## SAMPLE PREPARATION & MEASUREMENTS

### Materials

In this study, myristic acid (MA) is used as the base material and the graphene is selected to be additive in order to improve the thermal conductivity by composing a novel MA/Gr composite PCM. MA was purchased from Alfa Aesar has a

purity of 98% and graphene was obtained from Grafen Chemical Industries Company (Ankara, Turkey). The particle size, thickness and surface area of the Graphene is 5  $\mu\text{m}$ , 5-8 nm and 120-150  $\text{m}^2/\text{g}$ , respectively.

### Preparation of Myristic Acid/Graphene Composite PCMs

As a first step, myristic acid is heated to a temperature of 60°C in an incubator to ensure that MA is in the liquid phase and then graphene is added. After that, the mixture is subjected to an ultrasonic homogenizator (Misonix, Sonicator 3000) for approximately two minutes to procure homogeneous distribution. In order to determine the effect of graphene additive on the thermal conductivity of MA, the mass ratio of the graphene in the composite is varied to be 0.5%, 1% and 2%.

### Thermal Analyses

Perkin-Elmer Diamond TG/DTA is used to perform TGA analysis. The samples are observed from 25°C to 600°C at a heating rate of 10°C/min under nitrogen atmosphere. Besides, Perkin Elmer-Diamond DSC is used to determine the phase temperatures ( $T_m$  and  $T_f$ ) and latent heat values of melting ( $\Delta H_m$ ) and freezing ( $\Delta H_f$ ) for samples. The samples are scanned from 45°C to 65°C at a heating rate of 1°C/min and then the samples are held at 65°C for 1 min. After that, samples are cooled down from 65°C to 45°C at a rate of 1°C/min, and finally specimens are held at 45°C for 1 min.

### Thermal Cycling Tests

In order to reveal the thermal stability of composite PCMs DSC results are presented at the end of selected number of cycles such as 10, 40, 70, and 100. Thermal cycling tests are carried out with a constant scan rate of 5°C/min between 45°C and 65°C.

### Measurement of Thermal Conductivity

Thermal conductivity values of the PCMs are measured for the liquid phase. Instead of using a commercial instrument, a special experimental setup is designed on the basis of the 3- $\omega$  thermal conductivity measurement method. The method originates from the well-known hot-wire technique. A thin metal wire submerged into a liquid sample acts as a heater and thermometer. In the current setup, Ni wire with dimensions of 40  $\mu\text{m}$  in diameter and  $2l = 19.0$  mm long is used as a thermal probe (ThP). An alternating input current with a frequency of  $\omega$  heats the wire, consequently the sample with  $2\omega$  frequency. Since electrical conductivity of metal varies linearly with temperature, output voltage includes  $3\omega$  component which depends on thermal conductivity of the sample. The first harmonic in the voltage signal is dominant and must be cancelled by a Wheatstone bridge arrangement. The selection of the third harmonic from the differential signal across the bridge is performed by a Stanford SR850 lock-in amplifier tuned to this frequency [9] (Fig. 1). The method was validated with pure fluids, such as water, methanol, ethanol and ethylene glycol and yielding accurate thermal conductivity ratios within  $\pm 2\%$ . The main components of the experimental setup are illustrated on Figure 2. Further details about the setup and the theory of the 3-

$\omega$  thermal conductivity measurement method can be found elsewhere [8, 9].

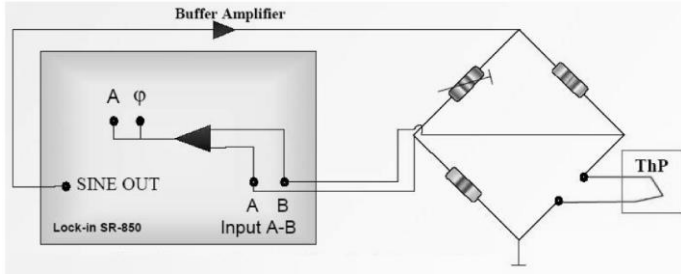


Figure 1 Schematic diagram of  $3\omega$  experimental set-up [9].

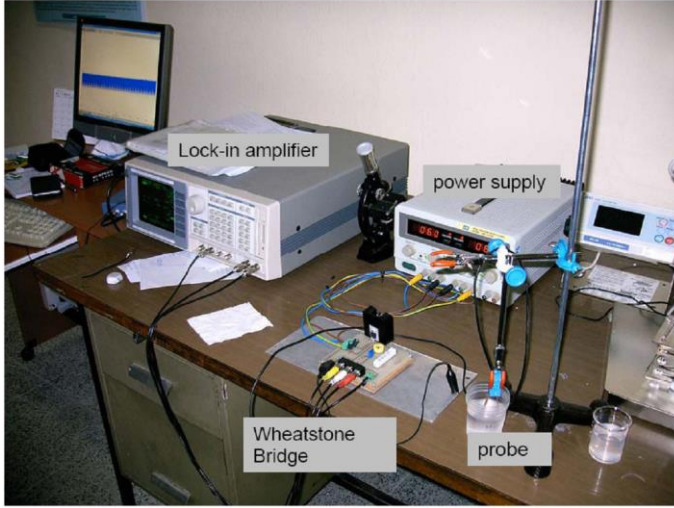


Figure 2 Main components of the  $3\omega$  experimental set-up [9].

## NUMERICAL STUDY

### Definition of the Problem

In order to reveal the influence of the increment in the thermal conductivity of MA on the phase change duration, some numerical investigations have been also conducted. In the analyses, it is assumed that PCMs (pure MA or composite MA/Gr) are encapsulated in a spherical enclosure with an initial temperature of  $T_{in}$  ( $T_{in} < T_m$ ). Then the sphere is suddenly submerged into a fluid (*water*) with a constant temperature of  $T_\infty$ . The outer diameter of the sphere is defined to be  $r_o = 14$  mm with a wall thickness of  $\delta r = 2$  mm. The schematic of the numerical model is illustrated in Figure 3.

### Governing Equations

The key limitation of the current analysis is that, the effect of natural convection has been neglected. Without the effect of natural convection, homogenous melting front may be expected. Therefore, the problem can be reduced into a one-dimensional heat conduction analysis. Hence, the corresponding energy equation can be written to be,

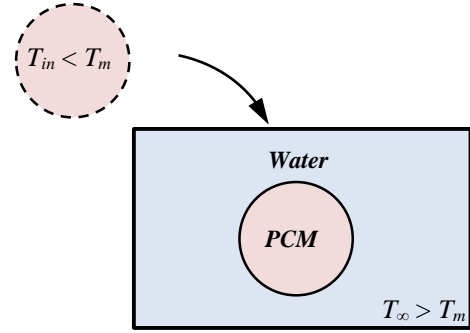


Figure 3 Definition of the numerical problem

$$\frac{\partial}{\partial t}(H) = \frac{1}{r^2} \frac{\partial}{\partial r} \left( kr^2 \frac{\partial T}{\partial r} \right) \quad (1)$$

In the current study, temperature transforming method of Cao and Faghri [10] has been implemented to simulate the phase change process. According to this method, enthalpy can be identified as a piece-wise linear functions in terms of temperature as,  $H = C^*T + S^*$ . Here the heat capacity ( $C^* = \rho c$ ) and source term ( $S^* = \rho s$ ) vary depending on the phase of the material (*liquid*, *mushy* or *solid*). Mushy region is a transition region which is limited by the temperature range of  $T_m \pm \delta T_m$ . The non-dimensional parameters are given in Table 1 are introduced to obtain dimensionless governing equation as

$$\frac{\partial}{\partial \tau}(C\theta) + \frac{\partial}{\partial \tau}(S) = \frac{1}{R^2} \frac{\partial}{\partial R} \left( KR^2 \frac{\partial \theta}{\partial R} \right) \quad (3)$$

where  $C$ ,  $K$  and  $S$  are defined for each phase of the material as follows,

$$C(\theta) = \begin{cases} C_s & \theta < -\delta\theta_m \\ 0.5(1+C_s) + \frac{1}{2Ste\delta\theta_m} & -\delta\theta_m \leq \theta \leq +\delta\theta_m \\ 1 & +\delta\theta_m < \theta \end{cases} \quad (4)$$

$$K(\theta) = \begin{cases} K_s & \theta < -\delta\theta_m \\ K_s + (1-K_s) \frac{\theta + \delta\theta_m}{2\delta\theta_m} & -\delta\theta_m \leq \theta \leq +\delta\theta_m \\ 1 & +\delta\theta_m < \theta \end{cases} \quad (5)$$

$$S(\theta) = \begin{cases} C_s\delta\theta_m & \theta < -\delta\theta_m \\ 0.5(1-C_s)\delta\theta_m + 0.5/Ste & -\delta\theta_m \leq \theta \leq +\delta\theta_m \\ C_s\delta\theta_m + 1/Ste & +\delta\theta_m < \theta \end{cases} \quad (6)$$

**Table 1** Dimensionless parameters

$C = (\rho c) / (\rho c)_L$	$K = k / k_L$
$S = (\rho c) / [(\rho c)_L (T_{in} - T_m)]$	$R = r / r_o$
$\theta = (T - T_m) / (T_{in} - T_m)$	$\tau = \alpha_L t / r_o$
$Ste = c_L (T_{in} - T_m) / \Delta H$	$Bi = hr_o / k_L$

## Solution Method

Governing equation is discretized into linear sets of algebraic equations with finite volume approach of Patankar [11]. Computational domain is divided into two hundred control volumes and stretched from the outer surface to the center of sphere to capture rapid phase change variation near the wall. In order to interpolate the variation of the thermal conductivity at the solid/liquid interface, harmonic mean thermal conductivity definition of Patankar [11] has been implemented. Tri-Diagonal Matrix Algorithm (TDMA) has been used to resolve the matrix. The computer code is developed in MATLAB programming language. As a result of the preliminary analyses the temperature range of the mushy zone, and time step size are selected to be  $T_m = 0.01^\circ\text{C}$  and  $t = 10$  s, respectively. Convergence criteria,  $\varepsilon$ , for each time step is defined in terms of the maximum relative change of temperature between two iterations for the whole domain, and for each time step  $\varepsilon < 10^{-14}$  is satisfied.

## RESULTS AND DISCUSSION

### Thermal Characteristics of PCMs

Results of the thermal cycling analyses are represented in Table 2 for the pure MA and MA/Gr composite PCMs. It is obvious that the graphene loading has no considerable effect on the melting or freezing temperature of the MA. Even for the greatest graphene fraction, the maximum variation is less than  $2^\circ\text{C}$ . It is also interesting that, for the pure MA, the degree of sub-cooling decreases with increasing thermal cycling. On the other hand, graphene loading suppresses the sub-cooling effect.

On contrary, increasing the amount of graphene fraction inside the composite PCM leads a reduction in the latent heat of melting and freezing values. In comparison to the pure MA, the melting and freezing enthalpy values decrease by almost 10% for the composite PCM with 2% graphene loadings.

DSC curves of the pure MA are derived at the end of 1<sup>st</sup>, 10<sup>th</sup>, 40<sup>th</sup>, 70<sup>th</sup> and 100<sup>th</sup> cycles and are represented in Figure 4. Results reveal that long term utilization of pure MA shifts the freezing temperature of MA. In contrast, no remarkable change is reported for the case of composite PCMs. These findings may indicate that, even for the highest graphene loading, the stability of the MA is not affected from the graphene treatment.

### Thermal Conductivity of PCMs

For each sample, five sets of measurements are carried out to determine the thermal conductivity values of the pure and composite PCMs. Thermal conductivity values of pure MA, MA/Gr0.5%, MA/Gr1% and MA/Gr2% are given in Table 3. It can be seen that increasing the fraction of graphene inside the composite PCM leads to increase in the thermal conductivity values, as expected. As the mass ratio of graphene increases from 0.5% to 2%, the increment in the thermal conductivity value raises from 8% to 38%.

### Thermal Stability of PCMs

DTG and TGA results for pure MA and composite PCMs are given in Figure 5 and Table 4. In terms of the TGA curves in Figure 5, one can see that for relatively lower graphene fractions, such as 0.5% and 1%, the curves differentiate from

pure MA. In contrast, for the highest graphene ratio, no significant difference is monitored. Results in Table 4 show that graphene loading does not cause any remarkable change in terms of the initial and maximum degradation temperatures of MA.

**Table 2** The effect of thermal cycling and graphene loading on the thermal properties of MA

Thermal cycling	Sample	$T_m$	$\Delta H_m$	$T_f$	$\Delta H_f$	$T_m - T_f$
		( $^\circ\text{C}$ )	(J/g)	( $^\circ\text{C}$ )	(J/g)	( $^\circ\text{C}$ )
1 <sup>st</sup> cycle	MA	56.0	202	53.7	-196	2.3
	MA/Gr0.5%	56.0	196	54.8	-195	1.2
	MA/Gr1%	54.8	183	53.7	-182	1.1
	MA/Gr2%	54.6	186	53.7	-182	0.9
10 <sup>th</sup> cycle	MA	55.7	200	53.9	-194	1.8
	MA/Gr0.5%	55.7	197	54.8	-194	0.9
	MA/Gr1%	54.7	186	53.8	-182	0.9
	MA/Gr2%	54.7	185	53.7	-180	1.0
40 <sup>th</sup> cycle	MA	55.7	200	54.0	-193	1.7
	MA/Gr0.5%	55.7	197	54.9	-193	0.8
	MA/Gr1%	54.7	186	53.8	-182	0.9
	MA/Gr2%	54.7	185	53.7	-180	1.0
70 <sup>th</sup> cycle	MA	55.7	198	54.1	-193	1.6
	MA/Gr0.5%	55.7	197	54.9	-193	0.8
	MA/Gr1%	54.7	186	53.7	-181	0.9
	MA/Gr2%	54.7	184	53.7	-180	1.0
100 <sup>th</sup> cycle	MA	55.7	198	54.3	-192	1.4
	MA/Gr0.5%	55.7	197	54.9	-193	0.8
	MA/Gr1%	54.7	186	53.8	-181	0.9
	MA/Gr2%	54.7	184	53.7	-180	1.0

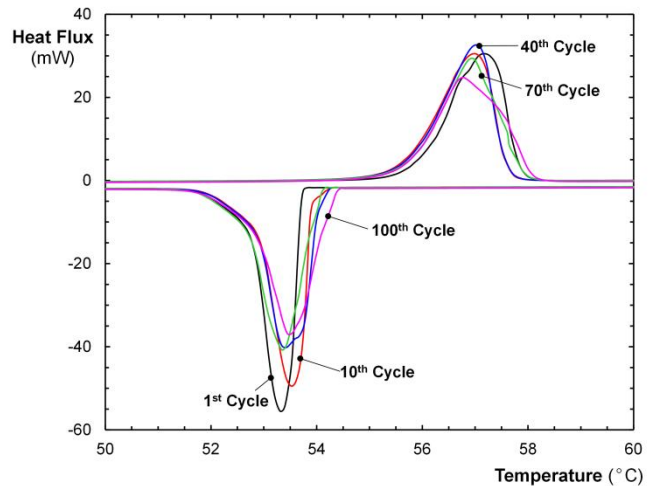


**Figure 4** DSC curves for Pure MA

**Table 3** Thermal conductivities of PCMs

Sample	Thermal conductivity (W/mK)	Standard Deviation
MA	0.15	$\pm 0.01$
MA/Gr0.5%	0.16	$\pm 0.01$
MA/Gr1%	0.18	$\pm 0.01$
MA/Gr2%	0.21	$\pm 0.01$

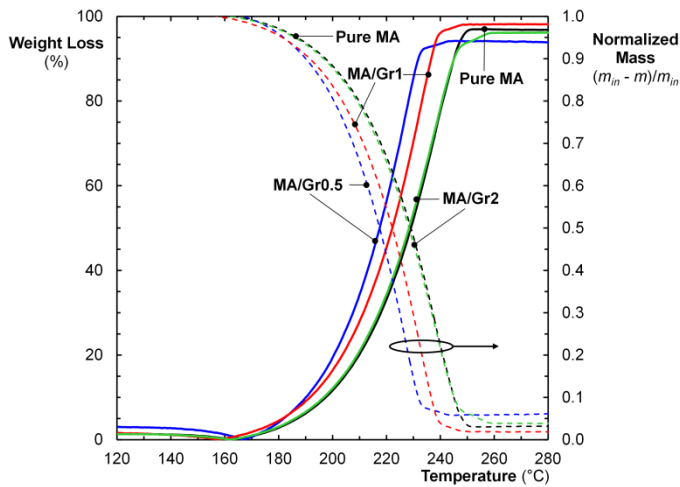


Figure 5 TGA curves for PCMs

Table 4 TGA Data for PCMs

Sample	Initial (°C)	End (°C)	Max. (°C)	Weight Loss (%)
MA	131	260	238	95.1
MA/Gr0.5%	125	254	227	90.0
MA/Gr1%	128	255	234	96.7
MA/Gr2%	131	262	240	95.0

### Validation of the Numerical Method

The validity of the numerical code is revealed by reproducing the numerical work of Bilir and Ilken [12]. For the validation case, a spherical container with an inner diameter of 0.06 m is considered. The spherical container is filled with water at 25°C, and then suddenly submerged into a tank which contains ethylene-glycol/water mixture at -25°C. Bilir and Ilken [12] assumed that the convective heat transfer coefficient around the sphere is  $h = 218.7$  (W/m<sup>2</sup>K) and remains constant for the whole process. Unlike the current study, in the reference work, enthalpy method of Vollmer [13] has been used to resolve the phase change. Time-wise variation of the surface temperature is represented in Figure 6 for the current and reference works. It is clear that, for the reference case, there are some oscillations in temperature values and the intensity of the oscillations diminishes in advancing time. Bilir and Ilken [12] stated that these oscillations may occur because of the implementation of harmonic mean definition for the thermal conductivity values at the interfaces of control volumes. In order to suppress temperature fluctuations, in the reference work, Bilir and Ilken varied the total number of control volumes from 11 to 41, and they have indicated that the temperature fluctuations reduce with increasing the number of total grid. In Figure 6, current predictions are compared with the finest mesh case of the reference work, namely 41. In the current analyses, number of mesh is selected to be five times higher than the reference work for each run, namely 200. Hence, no further attempt is made for optimization of the total number of grid.

On the other hand, as shown in Figure 6, time-step-size is varied to be 0.1 s, 0.5 s, 1 s, 5 s, and 10 s. Comparative results show that current predictions have no fluctuations and quite

close to the results reference work. It is reported that the mean deviation between the results of 0.1 s and 10 s is less than 1%. Hence, in order to consume less computational time for each parametric run, following analyses are carried out for  $dt = 10$  s.

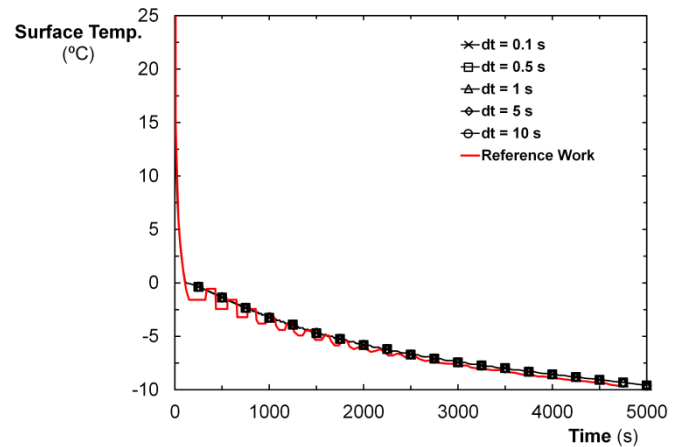


Figure 6 Validation of the numerical code

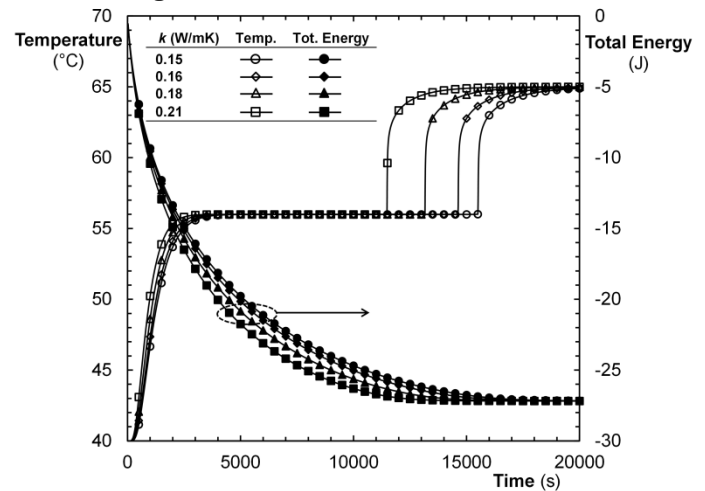


Figure 7 Effect of thermal conductivity on phase change

### Influence of Thermal Conductivity on Phase Change

In Figure 7, influence of thermal conductivity on the time-wise variations of center temperature and total energy are represented. Here, it should be noted that increasing the thermal conductivity considerably decreases the total melting time. In comparison to the pure MA, treatment of graphene in a mass ratio of 0.5%, 1%, and 2% decreases the total melting time by 5.6%, 15% and 26%, respectively.

### CONCLUSION

Since the duration of charging and discharging periods are limited for solar power, it is critical to finalize the process in a pre-determined time period. This study mainly focuses on increasing the thermal conductivity of a PCM (Myristic acid) which is suitable for moderate temperatures such as solar energy applications. Current findings reveal that graphene additives in Myristic Acid, even for smallest amounts, tend to increase the thermal conductivity of composite PCM and reduce the total phase change time without any significant

change in the remaining thermal properties, such as phase change temperature or latent heat. In contrary, it is introduced that the graphene treatment decreases the degree of sub-cooling. Thermal cycling results also proved that proposed composite PCMs are suitable for long term utilization.

## ACKNOWLEDGEMENT

The authors would like to acknowledge the support of the Scientific and Technological Research Council of Turkey (TUBITAK) under Grant No: 112M164.

## REFERENCES

- [1] Dincer, I., and Rosen, M., *Thermal Energy Storage: Systems and Applications*, John Wiley & Sons, 2002.
- [2] Kousksou, T., Bruel, P., Jamil, A., El Rhafiki, T., and Zeraouli, Y., Energy storage: Applications and challenges, *Solar Energy Materials & Solar Cells*, Vol. 120, 2014, pp. 59-80.
- [3] Sharma, S.D., and Sagara, K., Latent heat storage materials and systems: A review, *International Journal of Green Energy*, Vol. 2, 2005, pp. 1-56.
- [4] Sharma, A., Tyagi, V.V., Chen, C.R., and Buddhi, D., Review on thermal energy storage with phase change materials and applications, *Renewable & Sustainable Energy Reviews*, 13, 2009, 318-345.
- [5] Sari, A., Karaipekli, A., and Kaygusuz, K., Fatty Acid/Expanded Graphite Composites as Phase Change Material for Latent Heat Thermal Energy Storage, *Energy Sources, Part A*, Vol. 30, 2008, pp. 464-474.
- [6] Fauzi, H., Metselaar, H.S.C., Mahlia, T.M.I., Silakhori, M., and Nur, H., Phase change material: Optimizing the thermal properties and thermal conductivity of myristic acid/palmitic acid eutectic mixture with acid-based surfactants, *Applied Thermal Engineering*, Vol. 60 261-265, 2013.
- [7] Mehrali, M., Latibari, S.T., Mehrali, M., Mahlia T.M.I., Metselaar, H.S.C., Naghavi, M.S., Sadeghinezhad, E., and Akhiani, A.R., Preparation and characterization of palmitic acid/graphene nanoplatelets composite with remarkable thermal conductivity as a novel shape-stabilized phase change material, *Applied Thermal Engineering*, Vol. 61, 2013, 633-640.
- [8] Turgut, A., Sauter, C., Chirtoc, M., Henry, J., Tavman, S., Tavman, I., and Pelzl, J., AC hot wire measurement of thermophysical properties of nanofluids with  $3\omega$  method, *The European Physical Journal-Special Topics*, Vol. 153, 2008, 349-352.
- [9] Tavman, I., and Turgut, A., An investigation on thermal conductivity and viscosity of water based nanofluids. *Microfluidics Based Microsystems*, 2010, pp. 139-162
- [10] Cao, Y., and Faghri, A., A Numerical Analysis of Phase Change Problem including Natural Convection, *ASME Journal of Heat Transfer*, Vol. 112, 1990, pp. 812-815.
- [11] Patankar, S., *Numerical heat transfer and fluid flow*, Taylor & Francis, 1980.
- [12] Bilir, L., and Ilken Z., Total solidification time of a liquid phase change material enclosed in cylindrical/spherical containers, *Applied Thermal Engineering*, Vol. 25, 2005, pp. 1488-1502.
- [13] Voller, V.R., and Prakash, C., A fixed grid numerical modelling methodology for convection-diffusion mushy region phase-change problems, *International Journal of Heat and Mass Transfer*, Vol. 30, 1987, 1709-1719.